The Analysis of Processing Algorithms of Laser Doppler Signal in LabVIEW Software

I.O. Kozlov, E.A. Zherebtsov, A.I. Zherebtsova, A.V. Dunaev
Biomedical Photonics Instrumentation Group,
Scientific-Educational Center of Biomedical Engineering,
State University – Education-Science-Production Complex,
Oryol, Russia

***Abstract* — In this article the authors researches algorithms for signal processing of laser Doppler flowmetry. This study aims to find the best characteristics of the algorithm in terms of accuracy and dynamics for use in new laser Doppler flowmetry instruments.**

Keywords – laser Doppler flowmetry; model Bonner-Nossal; power spectral density; signal-to-noise ratio.

I. INTRODUCTION

At the present time, the method of laser Doppler flowmetry (LDF) is widely used for evaluating the intensity of peripheral blood flow in microvessels. The unit of measure for LDF is the "index of blood microcirculation" (Im) – a value which is expressed in terms of relative perfusion units, and is proportional to the average concentration of red blood cells and their average velocity. Physically, the term Im is the result of processing the variable signal from the photodetector, which is formed by photomixing signals from the reference and those shifted due to the Doppler effect frequencies (in the band from 1 Hz to 24 kHz). The time based changes of the registered LDF device perfusion signal contain two main components: constant and variable. The constant component is the average blood perfusion of the selected time interval. The variable component of the signal is caused by physiological factors regulating blood volume and reflects the frequency rhythms of blood flow regulation. Both components are important for the diagnostics of quite a number of diseases. Using indirect signs, the researcher can evaluate various diseases of the peripheral nervous system, which is responsible for microvasculature fluctuations [1-3]. However, currently this method is not particularly demanded in medical practice due to a number of challenges which are primarily associated with the absence of a unified processing algorithm of the laser Doppler flowmeter signal. Frequently, different studies use different normalizing values for the calculation of LDF results. This often creates difficulties when comparing these obtained results. There are significant differences in the implementation of the mathematical model, grounded in the fundamental work of Bonner and Nossal [4]. In this paper we present the research of processing algorithms of the laser Doppler signal for the comparison of their accuracy and dynamic characteristics.

This work was supported by the state task of the Ministry of Education and Science, Russian Federation, for the State University–Education-Science-Production Complex (basic part, no.310).

II. HARDWARE OF LASER DOPPLER FLOWMETER

The schematic diagram of an existing Laser Doppler Flowmeter prototype is shown in fig.1. The prototype comprises a laser, photosensor, 2-chanel signal amplifier and filter, a data acquisition card, and PC with visual programming environment NI LabVIEW installed. Firstly, emitted light is transferred to a biological object (BO). Second, the scattered and reflected light is converted by photosensor. Third, the signal is amplified in a custom electronic board. Fourthly, the signal is digitized by a data acquisition card. In conclusion, LabVIEW-based custom software performs mathematical processing in accordance with the analyses algorithms.

The major components of the LDF prototype are described below:

(1) Laser: the laser diode LPS-785-FC (THORLabs) is selected as a laser source. A special feature of this laser diode is the durability and high monochromatic radiation. Center wavelength λ: 785 nm, current consumption: 45 mA, output power: 10 mW.

(2) Photosensor consists of the photodiode and current-to-voltage converter. The FDSP series photodiodes (THORLabs) are selected for the detection of radiation. The current-to-voltage converter is made using OP-07 amplifier.

(3) Electronic board consists of two channels. Each channel functions as a filter and amplifier. AC and DC components of the photocurrent are separated and processed separately. The AC component is amplified on dual high-speed low-noise operational amplifier MC33078p. The DC component is amplified on two operational amplifiers OP-07.

(4) Data acquisitions card (DAQ): model NI USB-6211 [5].

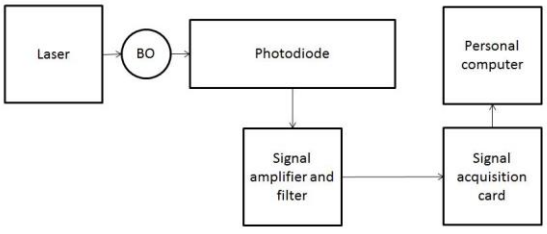

Fig. 1. Schematic diagram of the laser Doppler flowmeter

III. Algorithms of Processing Signal

The Doppler shift from moving particles can be evaluated by means of photocurrent analyses. There are many signal processing algorithms for LDF, based on the Bonner-Nossal model. In this study we discuss several algorithms of mathematical processing: Bonner-Nossal model normalized on the DC component of the photocurrent, Bonner-Nossal model normalized on the square of DC component of the photocurrent, Bonner-Nossal model normalized on the root mean square of the signal, Bonner-Nossal model normalized on the full energy of the signal, Bonner-Nossal model normalized on the sum of amplitudes of the spectra of the AC signal. The formulas of these algorithms are presented on Tab.1, where ω is the frequency offset, $S(U1(t)-U2(t))$ is the power spectrum density (PSD) of difference of the AC signals of two channels $U1(t), U2(t)$, ω1 and ω2 are the high-pass and low-pass cutoff frequencies, respectively [6-8].

TABLE I. Analyzed Algorithms of Signal Processing

Titles of algorithms	The formulas of algorithms
Bonner-Nossal model normalized on the sum of amplitude of the AC signal	$I_m = \frac{\int_{\omega 1}^{\omega 2} \omega \cdot S(U1(t)-U2(t))\,d\omega}{\int_{\omega 1}^{\omega 2} S(U1(t)-U2(t))\,d\omega}$
Bonner-Nossal model normalized on the root mean square of the AC signal	$I_m = \frac{\int_{\omega 1}^{\omega 2} \omega \cdot S(U1(t)-U2(t))\,d\omega}{RMS}$
Bonner-Nossal model normalized on the full energy of the signal	$I_m = \frac{\int_{\omega 1}^{\omega 2} \omega \cdot S(U1(t)-U2(t))\,d\omega}{RMS^2}$
Bonner-Nossal model normalized on the square of DC component of the photocurrent	$I_m = \frac{\int_{\omega 1}^{\omega 2} \omega \cdot S(U1(t)-U2(t))\,d\omega}{i_{dc}^2}$
Bonner-Nossal model normalized on the DC component of the photocurrent	$I_m = \frac{\int_{\omega 1}^{\omega 2} \omega \cdot S(U1(t)-U2(t))\,d\omega}{i_{dc}}$

IV. Analysis of Algorithms

Virtual instruments (VI) were built in the visual program environment LabVIEW. Software calculates the index of microcirculation by the algorithms discussed in Tab.1. Five basic tests were recorded on the middle finger of the left hand. The basic test has a five-minute record of LDF-gramm. Based on these data, statistical characteristics such as arithmetic mean, standard deviation and the coefficient of variation were calculated. In addition, occlusion tests were conducted as a ten-minute record of LDF-gramm during clamping of the upper arm by the cuff (Fig. 2). For this experiment we calculated the arithmetic mean, standard deviation and the evaluation of the signal-to-noise ratio. The arithmetic mean was calculated before the time of the occlusion test; the standard deviation was calculated during the time of the occlusion test. Signal-to-noise ratio was assessed as the ratio of the mean to the standard deviation.

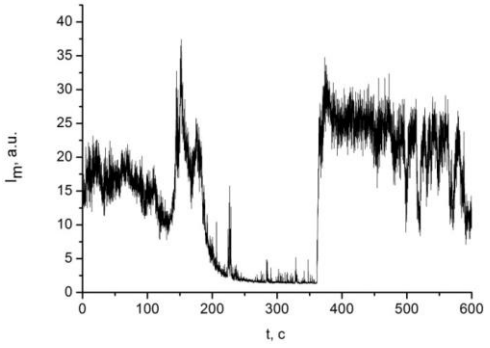

Fig. 2. LDF-chart of occlusion test

CONCLUSION

The main reason for the study is the identification of the models, which give the highest signal-to-noise ratio in occlusion test. Results of experiments are presented in Tab.2.

Bonner-Nossal model normalized on the DC component of the photocurrent and Bonner-Nossal model normalized on the square of DC component of the photocurrent proved to be the best models by the criterion of the signal-to-noise ratio. Thus, the inevitable presence of noise (hand and finger movements, noise of other nature) has a lower impact on these models.

TABLE II. EVALUATION OF THE SIGNAL-TO-NOISE RATIO

Titles of algorithms	Signal-to-noise ratio
Bonner-Nossal model normalized on the sum of amplitude of the AC signal	27.7
Bonner-Nossal model normalized on the root mean square of the AC signal	30.3
Bonner-Nossal model normalized on the full energy of the signal	3.3
Bonner-Nossal model normalized on the square of DC component of the photocurrent	40.0
Bonner-Nossal model normalized on the DC component of the photocurrent	38.8

Further, the study of mathematical models and their characteristics and the design of new relevant instruments are assumed.

REFERENCES

[1] A.I. Krupatkin, "Noninvasive estimation of human tissue respiration with wavelet analysis of oxygen saturation and blood flow oscillations in skin microvessels", Human Physiology, vol. 38, pp. 396-401, 2013.

[2] A.V. Dunaev, V.V. Sidorov, N.A. Stewart, S.G. Sokolovski, E.U. Rafailov, "Laser reflectance oximetry and Doppler flowmetry in assessment of complex physiological parameters of cutaneous blood microcirculation", Proc. SPIE. 8572, 857205, 2013.

[3] A.V. Dunaev, V.V. Sidorov, A.I. Krupatkin , I.E. Rafailov, S.G. Palmer, N.A. Stewart, S.G. Sokolovski, E.U. Rafailov, "Investigating tissue respiration and skin microhaemocirculation under adaptive changes and the synchronization of blood flow and oxygen saturation rhythms", Physiological Measurement, vol. 35(4), pp. 607-621, 2014.

[4] R. Bonner, R. Nossal, "Model for laser Doppler measurements of blood flow in tissue", Applied Optics, vol. 20, pp. 2097-2107, 1981.

[5] Hu, CL, Lin, ZS, Chen, YY, Lin, YH, Li, ML, "Portable Laser Doppler Flowmeter for Microcirculation Detection", Biomedical Engineering Letters, vol. 3(2), pp. 109-114, 2013.

[6] M.D. Stern, "Continuous measurement of tissue blood flow by laser-Doppler spectroscopy", American Journal of Physiology, vol. 232, pp. 441-448, 1977.

[7] I. Fredriksson, M. Larsson, F. Salomonsson, T. Stromberg, "Improved calibration procedure for laser Doppler perfusion monitors", Proc. SPIE 7906, 790602, 2011.

[8] A.N. Obeid, "In vitro comparison of different signal processing algorithms used in laser Doppler flowmetry", Medical and Biological Engineering and Computing, vol. 31(1), pp. 43-52, 1993.

[9] A.V. Dunaev, E.A. Zherebtsov, D.A. Rogatkin, N.A. Stewart, S.G. Sokolovski, E.U. Rafailov,"Substantiation of medical and technical requirements for noninvasive spectrophotometric diagnostic devices", Journal of Biomedical Optics, vol. 18(10), 107009, 2013.

[10] I.O. Kozlov, E.V. Zherebtsov, A.V. Dunaev, "New principles of construction devices for control of technical state of laser Doppler flowmetry monitors", Biotechnosphere, vol. 2(38), pp. 10-14, 2015.